

KINETIC STUDY OF BENTONITE-BASED DESULPHURISATION FOR CLEANER KEROSENE

Haider J. Esmaeel, Safaa M.R. Ahmed*

Department of Chemical Engineering, College of Engineering, Tikrit University, Iraq

*E-mail: safaamohamed@tu.edu.iq

ABSTRACT

This study introduces a novel, non-extractive Oxidative Desulphurisation (ODS) method for kerosene using a three-phase Oscillatory Baffled Reactor (OBR). The process utilises commercial bentonite clay (aluminium silicate hydrate) loaded with 15 wt% vanadium pentoxide (V_2O_5) as a cost-effective catalyst. Catalyst characterisation showed surface areas of $56 \text{ m}^2/\text{g}$ for bentonite and $50.13 \text{ m}^2/\text{g}$ for the V_2O_5 /bentonite composite. Structural and thermal properties were analysed using X-ray diffraction (XRD). The ODS process was tested under various conditions, including temperatures ($40\text{--}80^\circ\text{C}$), residence times (15–120 min), oscillation intensities (63.79–382.8 Reo), and sulphur concentrations (84.4–578 ppm). The optimal result, 81.73% sulphur removal, was achieved at 50°C , 578 ppm sulphur, and $\text{Reo} = 382.8$. Kinetic analysis revealed a second-order reaction with a low activation energy of 46.39 kJ/mol for dibenzothiophene (DBT) oxidation. Unlike previous studies that relied on synthetic or metal-heavy catalysts, this research highlights the effectiveness of a natural, low-cost bentonite-based catalyst. It offers a sustainable pathway for cleaner fuel production and contributes valuable insights into reaction mechanisms and kinetics, supporting future scale-up of eco-friendly desulphurisation technologies.

Keywords: Kerosene, desulphurisation, OBR, kinetic, vanadium pentoxide (v_2o_5), green fuel technology

INTRODUCTION

A crucial step in fuel refinement is desulphurisation, which lowers the sulphur content of petroleum products like gasoline, diesel, and kerosene. To comply with environmental regulations and enhance fuel quality, sulphur compounds naturally present in crude oil, such as thiophenes and benzothiophenes, must be eliminated. Acid rain, sulphur oxide (SO_x) production, and air pollution are all influenced by sulphur emissions [1]. Hydrodesulphurisation (HDS) has long been the most common technique for removing sulphur in refineries. Nevertheless, it is expensive and energy-intensive, requiring costly catalysts (Co-Mo and Ni-Mo on alumina), high pressure (30–130 atm), and high temperatures ($300\text{--}400^\circ\text{C}$). Furthermore, dibenzothiophene (DBT) and other refractory sulphur compounds are difficult for HDS to remove [2].

Because of its high surface area and ion exchange capabilities, bentonite, a naturally occurring clay rich in montmorillonite, has drawn interest as an affordable

catalyst and sorbent for removing sulphur. Oxidative Desulphurisation (ODS) is a process in which sulphur compounds react with an oxidising agent (such as hydrogen peroxide) in the presence of a catalyst to form more polar sulfoxides and sulphones that are easily extracted or adsorbed [3]–[4]. Benefits of bentonite-based ODS include lower operating pressures and temperatures, less hydrogen consumption, and high removal efficiency of refractory sulphur compounds. Understanding the process kinetics is necessary to improve catalyst performance, optimise reaction conditions, and scale up ODS for industrial applications. Kinetic models guide process optimisation for ultra-low sulphur by evaluating variables like reaction order, rate constants, and activation energy [5].

Although bentonite-based ODS shows promise, obstacles remain to effective and scalable sulphur removal. More efficient catalytic techniques are required due to the variability in oxidation efficiency among

sulphur compounds, especially refractory ones like 4,6-dimethyl dibenzothiophene (4,6-DMDBT) [6]. The availability of hydrogen peroxide and the catalytic activity of bentonite determine the reaction rate, necessitating careful control of temperature, reaction time, and oxidant concentration [7]. ODS usually takes place in a biphasic system, where the efficiency of the reaction is increased by improving the interfacial contact between kerosene and the oxidant through phase-transfer catalysts or emulsification techniques [8].

Oscillatory Baffled Reactors (OBRs) are ideal for ODS because they provide better reaction kinetics and increased mass transfer. In contrast to traditional stirred reactors, OBRs optimise the distribution of residence times by creating uniform shear fields through periodic oscillations inside a baffled structure. This process minimises undesirable side reactions and catalyst deactivation while increasing the efficiency of desulphurisation by improving contact between sulphur compounds and the oxidant. According to studies, oscillatory Reynolds number has a major impact on mixing performance, lowering energy consumption and speeding up sulphur conversion rates. OBRs are also suitable for industrial-scale applications since they allow continuous processing [9].

This work uses bentonite to create a thorough kinetic model for kerosene's ODS in an OBR. The study tries to create a pseudo-second-order kinetic model to explain adsorption and oxidation mechanisms while assessing the effects of operating parameters (temperature, residence time, and oxidant concentration). The results will help create a desulphurisation process that is energy-efficient, sustainable, and compliant with environmental standards [10].

EXPERIMENTAL PROCEDURE

Chemicals

The study utilised treated kerosene as the feedstock, characterised by a total sulphur content of 9 ppm, and supplied by the Midland Refineries Company, Dora Refinery. The detailed physical properties of the feedstock are listed in Table 1. Aluminium silicate hydrate (bentonite, 99%) was procured from Sisco Research Laboratories, Maharashtra, India, and hydrogen peroxide (H₂O₂), serving as the oxidising agent, was obtained from Merck Millipore, Germany.

Table 1 Specifications of kerosene

Physical property	Value
Specific gravity@15.5°C	0.8
API @15.6°C	48.2
Total sulphur (ppm)	9
Flashpoint, (°C)	~38
Pour point, (°C)	-25.1
Colour	30
Kinematic viscosity@40°C (mm ² /sec)	2.39
Initial boiling point (°C)	162
Distillation, (°C)	
10%	178
50%	196
90%	218
Final boiling point (°C)	244

Preparation of the Catalyst

25 g of dry bentonite was refluxed with 150 mL of 0.1 N HCl at 70°C for 3 hours to activate bentonite. After filtering, washing, and overnight drying, the mixture was calcined for five hours at 500°C. Because it effectively removed moisture and organic matter while preserving the bentonite's structural integrity, a calcination temperature of 500°C was used. The surface area and porosity of the material are improved at this temperature, which is important for both catalytic and adsorptive performance in desulphurisation applications. On the other hand, less activity and structural deterioration could result from greater calcination temperatures. After calcination, a solution of 15 wt% NH₄VO₃ in 50 millilitres of 1 M oxalic acid was prepared, agitated for an hour, and combined with 85 wt% bentonite at 50°C for two hours to create the V₂O₅/bentonite catalyst. After that, the oxalic acid was evaporated for an hour at 100°C. After being dried for 24 hours at 90°C, the mixture was sieved and then calcined for 5 hours at 500°C at a rate of 2°C per minute.

Reactor Assembly

Using a custom-built OBR system, as shown in Figure 1, we could remove sulphur from DBT. The OBR unit used in this study is fully automated and has a thermostat that controls the temperature. It is designed to improve mixing and mass transfer when the net flow is low, which is important for making reactions work better in liquid-phase processes. The main part of the system is a vertical cylindrical reactor that is 8 mm wide, 38 cm tall and has a total internal volume of about 19 mL. A helical baffle insert was put within the reactor

tube along its length to make mixing more effective. This baffled shape was chosen to encourage chaotic advection and improve the residence time distribution of reactants, which will help create a more even reaction environment along the length of the reactor.

System Setup

The oscillatory motion within the reactor was generated by a programmable syringe pump (Confluent PVM), which delivers precisely controlled harmonic displacements of the working fluid. The amplitude and frequency of oscillation could be adjusted independently to achieve optimal oscillatory Reynolds numbers (Re_o), which are known to critically influence the flow regime and mixing dynamics within OBRs. The reactor was surrounded by a high-efficiency electric heating jacket, providing uniform thermal energy along the reactor wall. The reactor's temperature was monitored and maintained using a digital PID temperature controller with an accuracy of $\pm 0.1^\circ\text{C}$. The entire assembly was thermally insulated using ceramic fibre material to minimise external heat losses and ensure consistent thermal conditions throughout the experimental runs.

All system components, including the reactor, pump, heating unit, and data acquisition interface, were integrated into a single automated platform, allowing for real-time monitoring and control of critical process

parameters such as oscillation frequency, stroke length, reaction temperature, and reaction time. The DBT-containing model oil was then introduced into the reactor under continuous oscillation, and samples were collected at specified time intervals for subsequent analysis.

The tubular reactor is fabricated from 316-grade stainless steel, chosen for its excellent corrosion resistance, mechanical strength, and compatibility with elevated temperatures and reactive chemical environments. The catalyst employed in this study is natural bentonite, selected for its high surface area, thermal stability, and adsorption capacity, which collectively enhance the desulphurisation process's overall efficiency. The key geometrical and design parameters of the reactor, including internal diameter, length, volume, and baffle configuration, are summarised in Table 2.

Table 2 Dimensions of the OBR

Dimension	Values
Tube diameter (D), mm	8
Tube height (h), cm	38
The wall thickness of the tube, mm	1
Tube volume (V), mL	19

Reaction Initiation

Using a syringe or a feed pump, inject the DBT feed solution into the reactor, ensuring there is no trapped air and the reactor is filled. To create oscillatory flow, turn on the syringe pump following the preset settings after correctly filling the reactor. Start heating the reactor and carefully monitor the temperature until it reaches and stays at the desired set point. Ensure a steady temperature and continuous oscillation are maintained during the reaction period.

Sampling and Analysis

At regular intervals, such as every ten minutes, liquid samples should be taken from the reactor exit. The samples should be quenched immediately if needed to stop the reaction process. The ASE-2 X-ray sulphur analyser from Bourevestnik in Russia was then used to measure the sulphur content of the samples according to the described analytical technique. The difference between the starting and final DBT concentrations can be used to calculate the DBT conversion value.

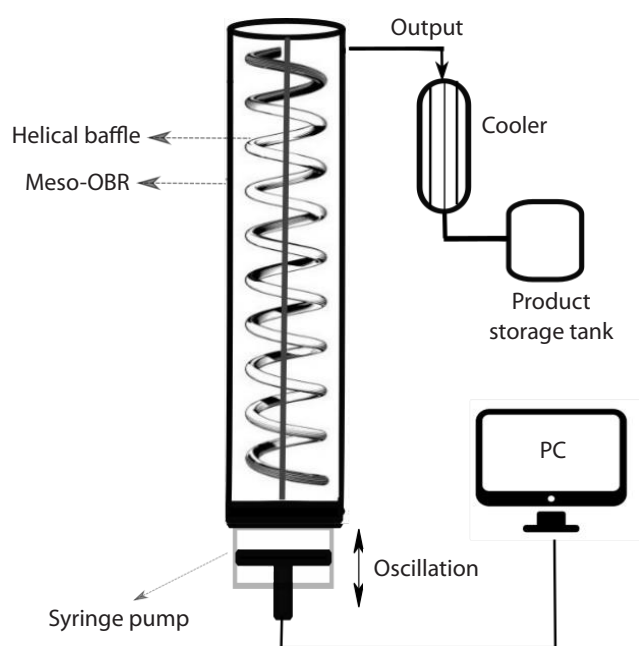
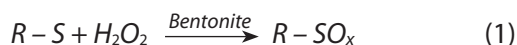


Figure 1 A scheme of the ODS system

Experimental Methods: ODSProcess

Chemical Reaction

The ODS process involves sulphur removal from kerosene using hydrogen peroxide (H₂O₂) and bentonite catalyst. The key reaction is:



where:

R-S = Sulphur-containing compounds (e.g., thiophenes, dibenzothiophenes),

H₂O₂ = Oxidising agent,

Bentonite = Catalyst and adsorbent,

R-SO_x = Oxidised sulphur compounds (sulphones/sulphoxides).

Operating Conditions

The main operating parameters examined during the ODS of kerosene in an OBR are compiled in and the effect of hydrodynamics was evaluated using varying Re_o of 127.6, 255.2, and 382.8 to assess mixing intensity and mass transfer enhancement.

As shown in Table 3, the kerosene flow rate was adjusted between 10 and 100 mL/min to imitate various

Table 3 Operating conditions

Parameter	Value
Kerosene Flow Rate, mL/min	10–100
Sulphur Content, ppm	84.4, 177, 578
H ₂ O ₂ Concentration, wt%	30–50
Bentonite Concentration, g/L	1–10
Temperature, °C	40, 50, 80
Pressure, bar	1
Space-time, min	15, 30, 60, 120
Oscillatory baffled, Re _o	127.6, 255.2, 382.8

fuel grades, while the feed’s sulphur concentration was adjusted between low (84.4 ppm) and high (578 ppm). Bentonite was employed as the catalyst, with concentrations ranging from 1 to 10 g/L, and hydrogen peroxide (H₂O₂) was employed as the oxidant, with concentrations ranging from 30 to 50 wt%. Various temperatures (40°C, 50°C, and 80°C) and atmospheric pressure (1 bar) were used for the experiments. The reactor’s residence time (also known as space-time) was varied from 15 to 120 minutes, and the effect of hydrodynamics was evaluated using varying Re_o of 127.6, 255.2, and 382.8 to assess mixing intensity and mass transfer enhancement.

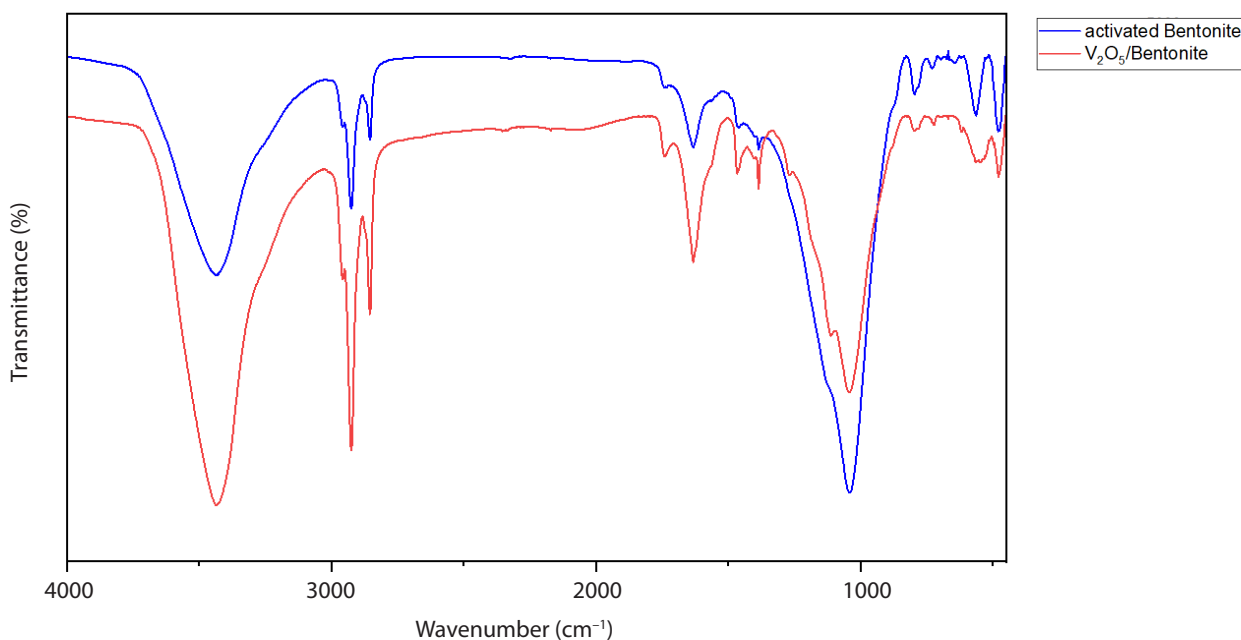


Figure 2 FTIR results for bentonite support and V₂O₅-bentonite catalyst

RESULTS AND DISCUSSION

Catalyst Characterisation Results

Fourier Transform Infrared Spectroscopy (FTIR)

Results

The FTIR spectrum compares activated bentonite (blue line) and V₂O₅-loaded bentonite (red line) (Figure 2), highlighting structural changes upon vanadium oxide incorporation.

The broad peak around 3400 cm⁻¹, attributed to O-H stretching of hydroxyl groups and water molecules, decreases in intensity after vanadium loading, indicating interactions between V₂O₅ and surface hydroxyls [11]. The peak near 1630 cm⁻¹, corresponding to the H-O-H bending of adsorbed water, shows changes suggesting variations in hydration. The strong bands between 1100-400 cm⁻¹, characteristic of Si-O-Si and Si-O-Al vibrations in the bentonite structure, exhibit shifts or intensity variations due to V₂O₅ deposition [12]. Additionally, new peaks or shifts around 800–1000 cm⁻¹, corresponding to V=O and V-O-V stretching vibrations, confirm the presence of vanadium oxide. These spectral modifications collectively indicate the successful incorporation of V₂O₅ onto the bentonite surface, altering its chemical and structural properties.

Brunauer–Emmett–Teller (BET) Results

Figure 3a and 3b present adsorption/desorption isotherms derived from BET analysis for two materials: (a) activated bentonite and (b) V₂O₅-bentonite catalyst.

The isotherms illustrate the relationship between the relative pressure (p/p_0) and the adsorbed volume (V)

of nitrogen gas at STP per gram of material [13]. The blue diamond markers represent the adsorption (ADS) process, while the red square markers indicate the desorption (DES) process. Both isotherms exhibit a characteristic Type IV behaviour, typically associated with mesoporous materials, indicating the presence of capillary condensation [14]. The noticeable hysteresis loop between adsorption and desorption curves suggests the presence of slit-like or cylindrical mesopores, which are common in catalysts and adsorbents with high surface area. The BET surface area for Activated Bentonite is 56 m²/g, whereas the V₂O₅-Bentonite Catalyst has a slightly lower BET surface area of 50.134 m²/g. Despite this slight decrease in surface area, the modified catalyst shows increased nitrogen uptake at higher relative pressures, suggesting improved porosity and structural modification due to V₂O₅ incorporation. These results highlight the structural and textural differences between the two materials, which are crucial for their adsorption efficiency and catalytic performance.

Effect of Process Parameters

Effect of Temperature

Figure 4a-4c illustrate the effect of temperature on the ODS performance of the V₂O₅-bentonite catalyst under varying process conditions, space-time; $\tau=120$ min, oscillation conditions (63.3, 127.6, 255.2, and 382.8), and initial DBT concentration of 84.4 ppm (a), 177.7 ppm (b), and 578 ppm (c).

Figure 4 illustrates the influence of reaction temperature on the conversion of sulphur compounds at a constant reaction time of 120 minutes across three different initial DBT concentrations (578 ppm, 177.7 ppm, and

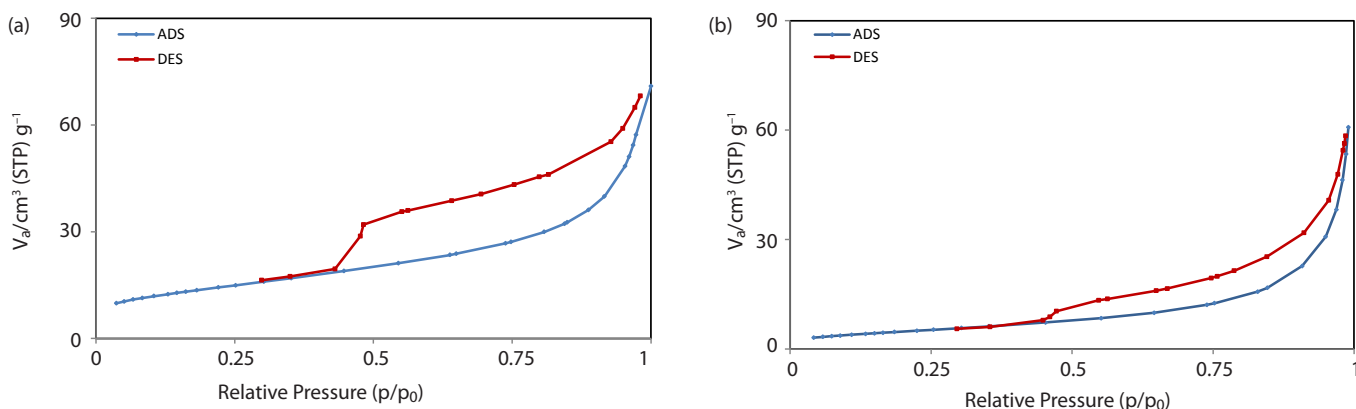


Figure 3 Adsorption/desorption isotherm for BET results: a) Activated bentonite, and b) V2O5-bentonite catalyst

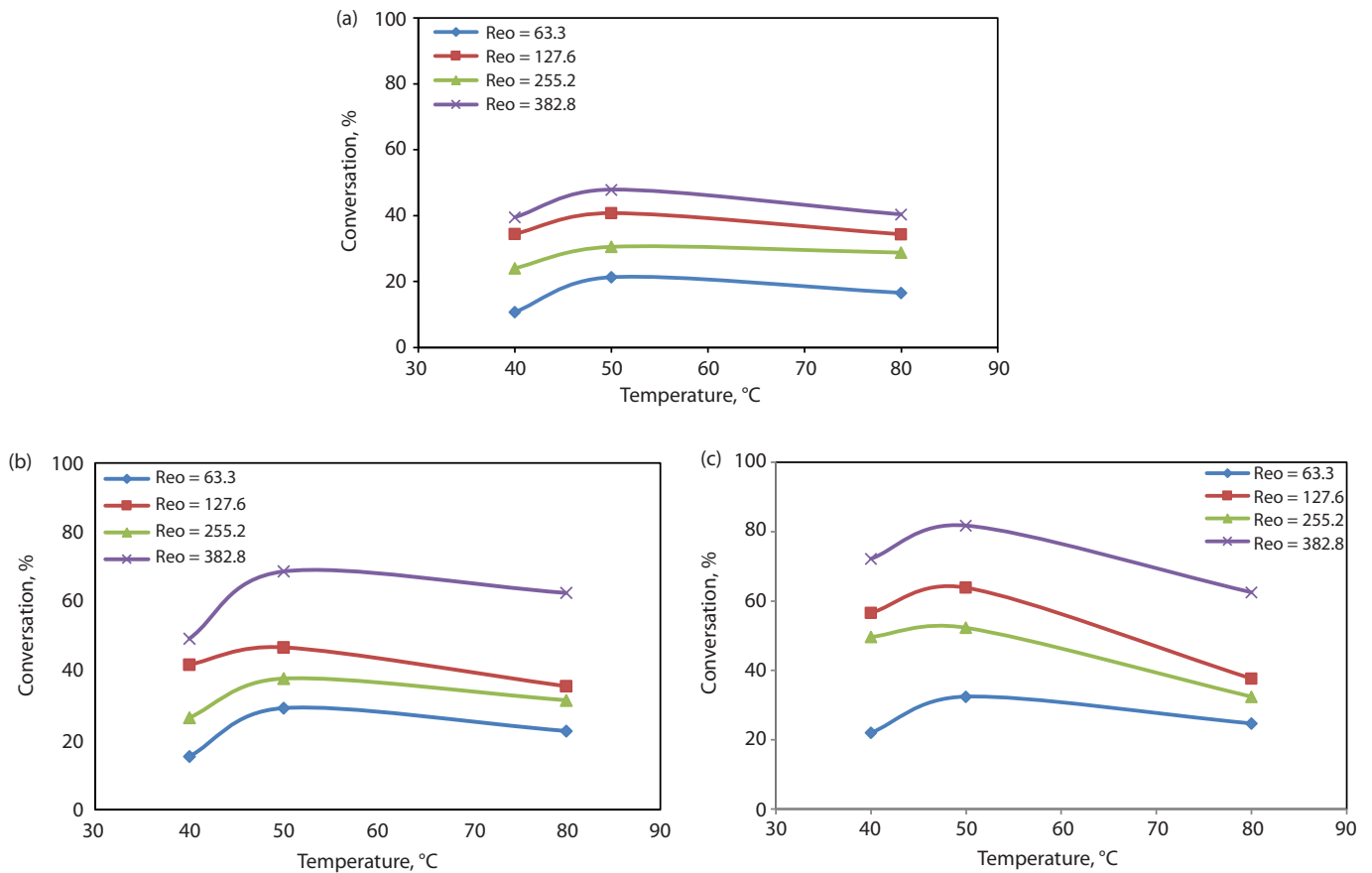


Figure 4 Effect of temperature on the process conversion at $\tau=120$ min, and initial DBT concentration a) 84.4 ppm, b) 177.7 ppm, and c) 578 ppm

84.4 ppm). The results demonstrate a clear positive correlation between temperature and sulphur conversion efficiency. This enhancement can be attributed to several interrelated factors.

The reaction kinetics of the ODS process become faster when the temperature rises. Higher temperatures reduce the activation energy barrier, as the Arrhenius equation states, which causes more effective collisions between DBT molecules and oxidising agents. The oxidation process transforms sulphur species into sulphones more rapidly and efficiently because sulphones separate more readily from the hydrocarbon matrix [15]-[16].

The intrinsic activity of the V_2O_5 -bentonite catalyst rises at higher temperatures due to improved movement and reaction rates of surface oxygen species. The application of thermal energy helps to distribute V_2O_5 more evenly throughout the bentonite structure, leading to more available active sites and improving catalytic efficiency [17].

The observed conversion improvement at increased Reynolds numbers underscores enhanced mass transfer effects. Increased turbulence enhances DBT molecule delivery to catalyst surfaces while facilitating reaction product removal to reduce external diffusion limitations [18]. Initial DBT concentrations at reduced levels produce elevated sulphur conversion percentages. The catalyst demonstrates increased efficiency under conditions where active sites remain unsaturated, enabling more effective oxidation processes at reduced sulphur loadings. The overall reaction efficiency faces obstacles at higher concentrations due to restricted active site availability and competitive adsorption [19]. According to these findings, the V_2O_5 -bentonite catalyst performance depends heavily on temperature and hydrodynamic conditions. Parameter optimisation is critical to enhancing ODS process efficiency while attaining fuel cleanliness through lowered sulphur content.

Effect of Space-time

Figures 5a-5c show the effect of space-time on the reaction conversion at $T=50^{\circ}\text{C}$, oscillation conditions (63.3, 127.6, 255.2, and 382.8), and initial DBT concentration of 84.4 ppm (a), 177.7 ppm (b), and 578 ppm (c).

The results show a strong relationship between increased space-time and improved conversion, indicating that longer residence times facilitate better interaction between the reactants and the V_2O_5 -bentonite catalyst, promoting ODS. Longer contact times have been found to favour higher sulphur removal efficiency by increasing the likelihood that DBT molecules will reach and react on catalytically active sites [20]-[21]. This behaviour is consistent with findings in the literature.

Furthermore, the findings show that increased Re_o enhance conversion efficiency at all concentrations, underscoring the critical role that enhanced mixing and mass transfer play in promoting the oxidation

reaction. Mass transport to and from the catalyst surface is improved by oscillatory flow, which increases turbulence and reduces the diffusion boundary layer [22].

At lower initial sulphur concentrations (Figure 4a), the conversion reaches almost 100% quickly, which means that the catalyst works better when the sulphur loading is lower. This is because there are more active catalytic sites than sulphur-containing molecules, which makes competitive adsorption less effective [23]. On the other hand, the conversion happens more slowly at higher initial concentrations (Figures 4b and 4c), so the reaction needs more time to reach the same level of desulphurisation. As this trend shows, longer residence times are needed to ensure enough oxidation when there is more pollution.

The trends show how hydrodynamic conditions and reaction kinetics work together. For example, higher oscillatory flow conditions (higher Re_o) make turbulence worse and lower mass transfer constraints,

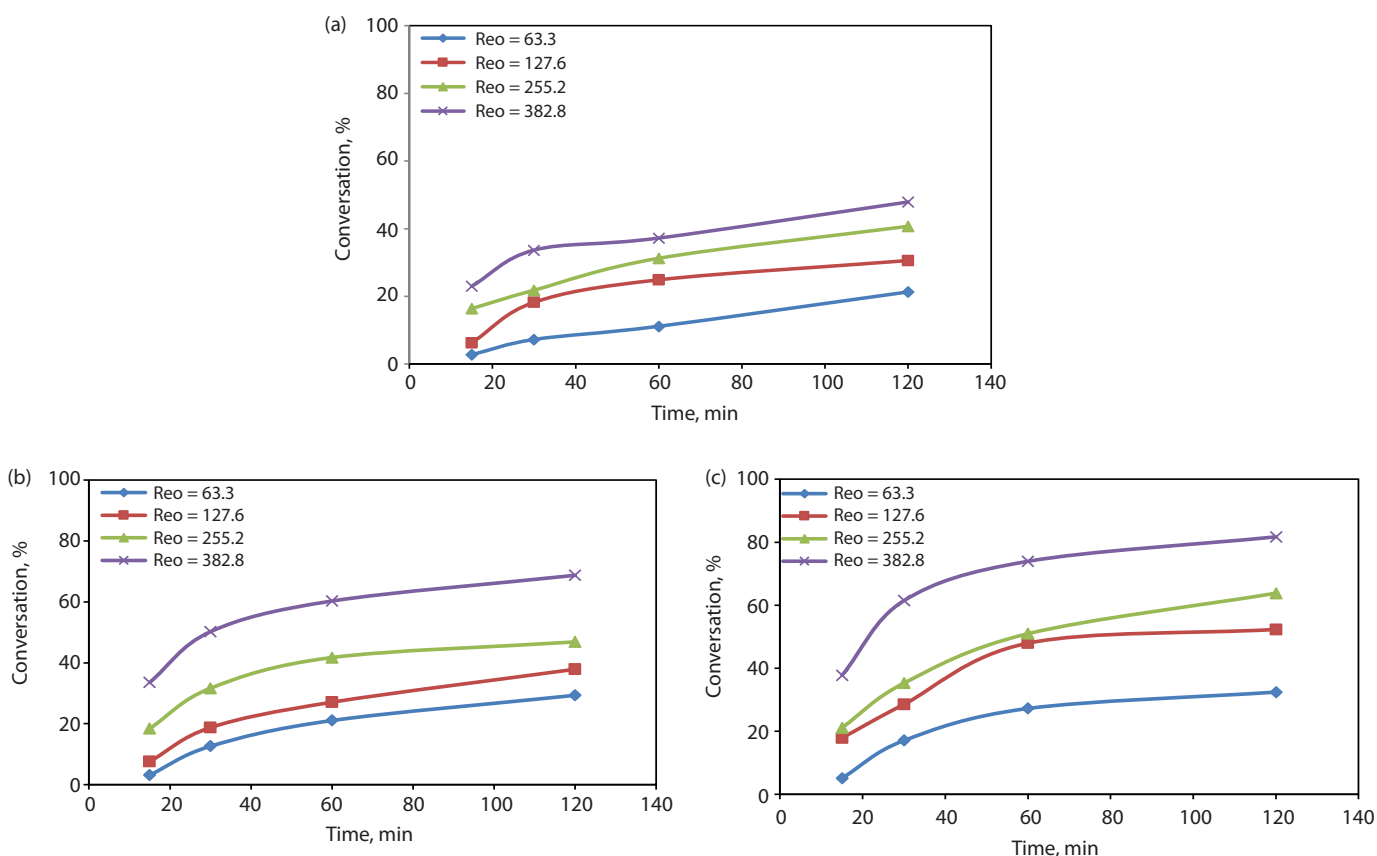


Figure 5 Effect of space-time on conversion at $T=50^{\circ}\text{C}$, and initial DBT concentration a) 84.4 ppm b) 177.7 ppm c) 578 ppm

which speed up the oxidation process. These results show the importance of getting the most sulphur removal efficiency by fine-tuning space-time and oscillatory flow parameters. Hence, making the V₂O₅-bentonite catalyst a good choice for advanced ODS applications.

Kinetic Analysis

The Kinetic Study of the ODS Process in an OBR

The following presumptions were made to model the kinetics of DBTs ODS precisely:

1. **Isothermal Reaction Conditions:** The temperature and reaction volume stay constant throughout the reaction. This guarantees that the rate constant *k* won't change throughout the process.
2. **Constant Catalyst Activity:** It is anticipated that the V₂O₅-bentonite catalyst will continue to exhibit stable activity throughout the reaction. Deactivation of the catalyst (for example, by fouling or leaching) is disregarded.
3. **No Mass Transfer Limitations:** DBT diffusion to or within the catalyst particles is not thought to influence the observed reaction rate, which is thought to be entirely controlled by chemical kinetics. This is supported by using suitable Reynolds numbers, such as *Re*₀ = 382.8, which suggests efficient mass transport and mixing.
4. **Minimal Volume Change During Reaction:** The integration technique's mass balance equations are simplified by assuming that the reaction mixture's total volume stays constant.
5. **Pseudo-homogeneous Reaction:** This allows for consistent reaction rate expressions throughout the volume by simplifying the catalyst's heterogeneous nature into a pseudo-homogeneous system.
6. **Reaction Follows a Single Rate-Determining Step:** Simple power-law kinetics can be used for rate modelling since a single elementary step is assumed to dominate the reaction mechanism.
7. **No Side Reactions:** Only the intended oxidation reaction is considered. Parallel reactions or the creation of undesirable byproducts are disregarded.

The kinetic study of the ODS reaction was carried out according to the experimental results at *Re*₀ = 382.8, initial concentration = 578 ppm, and spatial time range from 15 to 120 min. In this work, the rate law of the DBT

oxidation reaction was estimated from experimental data using the integration technique. The integration analysis technique guessed and incorporated a reaction order into the integration process. An alternative rate equation is proposed and evaluated when the concentration or conversion profiles deviate from the expected behaviour, equated as:

$$-r_{DBT} = -\frac{dC_{DBT}}{dt} = k C_{DBT}^n \quad (2)$$

Assuming a first-order rate equation (*n* = 1), the general rate expression simplifies to:

$$-r_{DBT} = -\frac{dC_{DBT}}{dt} = k C_{DBT}^1 \quad (3)$$

Upon separation and integration of the rate expression:

$$-\int_{C_{DBT0}}^{C_{DBT}} \frac{dC_{DBT}}{C_{DBT}} = k \int_0^t dt \quad (4)$$

$$\ln \frac{C_{DBT0}}{C_{DBT}} = kt \quad (5)$$

Similarly, the second-order rate equation (*n* = 2) was used to derive the following expression:

$$\frac{1}{C_A} - \frac{1}{C_{A0}} = kt \quad (6)$$

where:

*r*_{DBT} = rate of DBT oxidation reaction, (mol/L. min)

K = Reaction rate constant, (min⁻¹)

*C*_{DBT0} = Initial concentration of DBT (inlet concentration of DBT into the reactor), (mol/L)

*C*_{DBT} = Outlet concentration of DBT from the reactor (mol/L)

t = reaction time, (min)

n = reaction order

Figures 7 and 8 were obtained by fitting the experiment results of the plot of ln(C_{DBT0}/C_{DBT}) versus reaction time and the plot of (1/C_A-1/C_{A0}) versus reaction time.

Figure 6 and Figure 7 presents the kinetic analysis of a reaction using first-order and second-order models at three different temperatures (40°C, 50°C, and 80°C). Figure 6 plots ln (C₀/C) versus time, representing the first-order model, while Figure 7 plots (1/C - 1/C₀) versus time, representing the second-order model. Each dataset is fitted with a linear regression equation, with the corresponding R² values indicating the goodness of fit for each kinetic model.

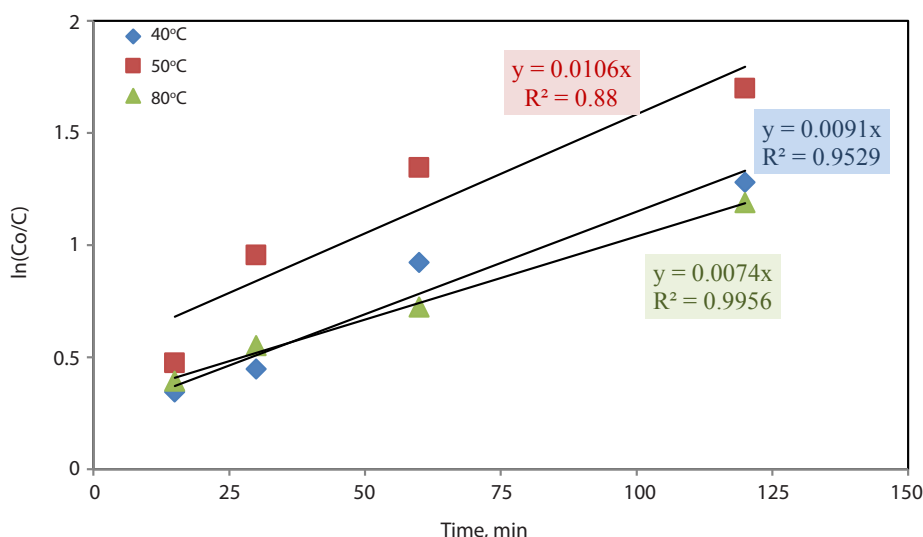


Figure 6 Kinetic data representation using first-order rate

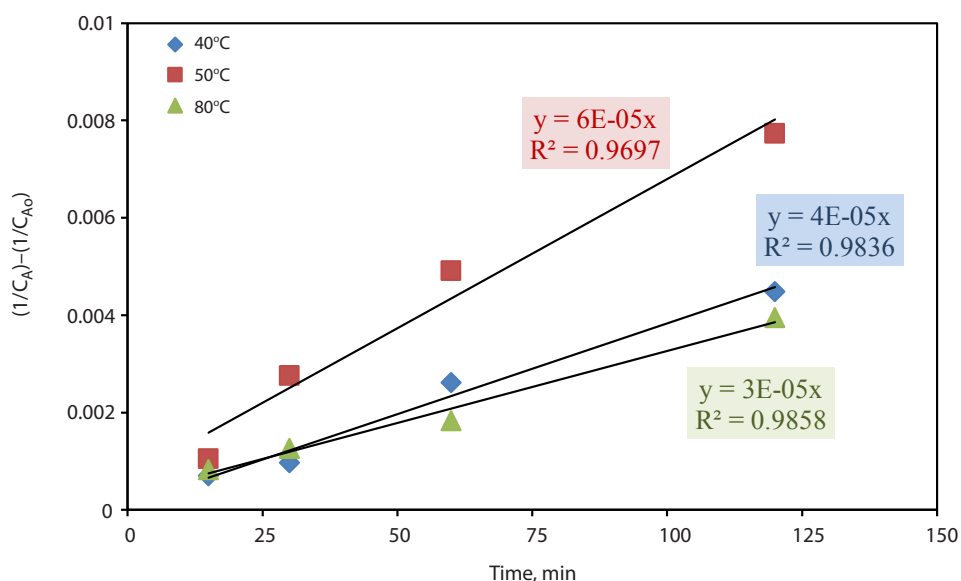


Figure 7 Kinetic data representation using second-order rate

In the first-order model, the reaction rate constant (k) increases with temperature, confirming the temperature dependence of reaction kinetics. The highest reaction rate is observed at 80°C ($k=0.0106$), followed by 50°C ($k=0.0091$) and 40°C ($k=0.0074$), with high R^2 values (0.88–0.9956), suggesting a strong fit to the model. A similar trend is observed in the second-order model, with reaction rates increasing at higher temperatures. The rate constants at 80°C, 50°C, and 40°C are $6E-05$, $4E-05$, and $3E-05$, respectively. The R^2 values (0.9697–0.9858) indicate a good correlation between the data and the second-order model.

By comparing the R^2 values, it is evident that both kinetic models describe the reaction well. Still, the second-order model provides a slightly better fit for lower temperatures, where R^2 values are closer to 1. However, in Figure 7, the second-order model demonstrates a strong fit, indicating that the reaction mechanism may shift towards second-order kinetics at higher temperatures. This suggests that the reaction kinetics are temperature-dependent and may follow a mixed-order behaviour under varying conditions.

The activation energy for the oxidation of DBT can be determined from the slope of the Arrhenius plot (Figure 8) using the linearised form, defined as:

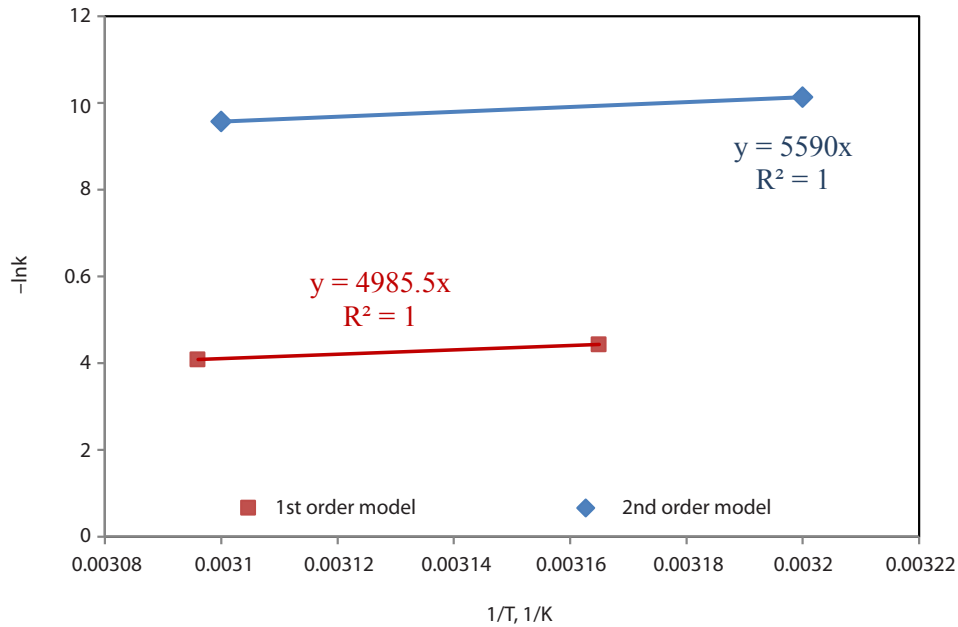


Figure 8 Temperature dependency of DBT oxidation reaction according to Arrhenius’ law

$$-\ln k = -\ln k_0 + \frac{E}{RT} \quad (7)$$

where, T is the reaction temperature (K), R is the gas constant (kJ/mol.K), E is the Activation energy (kJ/mol), and k_0 is the Pre-exponential factor (-).

The Arrhenius plots for DBT oxidation using $-\ln(k)$ versus $1/T$, examined for both first- and second-order kinetics, are shown in Figure 8. The Arrhenius equation within the examined temperature range is validated by the strong linearity of the two data points provided for each model. Practical difficulties are the source of the data points’ limitation: a decrease in conversion was noted at 80°C, most likely due to oxidant degradation that produced non-physical rate constants. On the other hand, conversion was too low at lower temperatures to yield useful rate values within a

feasible experimental range. Despite the small number of points, the calculated activation energy (46.39 kJ/mol) is dependable and within the anticipated range for catalytic ODS systems. This value is much lower than those reported for uncatalysed ODS reactions (85-89.7 kJ/mol) and conventional HDS processes (96.5-104 kJ/mol), which require more energy, as Table 5 clarifies. The V_2O_5 -bentonite catalyst provides a balanced combination of moderate activation energy and operational simplicity compared to other sophisticated ODS techniques such as photocatalysis (~30 kJ/mol) or formic acid oxidation (59.8 kJ/mol). This method demonstrates that meaningful and comparative kinetic insight has been achieved even with limited data, reinforcing the practical significance of the data points included.

Table 4 Summary of the kinetic data

Model / Operating conditions	$T = 40^\circ\text{C}$	$T = 50^\circ\text{C}$	$T = 80^\circ\text{C}$	
Pseudo-first order kinetic model	$k = 0.0091$ $R^2 = 0.95$	$k = 0.016$ $R^2 = 0.88$	$k = 0.0074$ $R^2 = 0.9956$	$E = 28.5 \frac{\text{kJ}}{\text{mol}}$
Pseudo-second order kinetic model	$k = 0.00004$ $R^2 = 0.983$	$k = 0.00006$ $R^2 = 0.9697$	$k = 0.00003$ $R^2 = 0.9858$	$E = 46.39 \frac{\text{kJ}}{\text{mol}}$

Table 4 summarises the obtained data from the kinetic study for both first and second-order models.

Comparison with Other Desulphurisation Techniques for Kerosene ODS

Table 5 presents a comparative analysis of the kerosene ODS results obtained in this study against findings from previous research.

The ODS of kerosene in the current study using an OBR is thoroughly compared with other desulphurisation methods, such as ODS, HDS, and biodesulphurisation (BDS), in Table 5. Important factors like the sulphur compound (e.g. DBT), reactor types, oxidants or catalysts, kinetic models, and activation energies are the main focus of the comparison. The current study highlights a more effective reactor design and an eco-friendly catalytic system’s moderate activation energy of 46.39 kJ/mol using H₂O₂ with V₂O₅-bentonite in an OBR. The ODS-OBR approach is more energy-efficient and operationally safer because this energy is substantially lower than reported for HDS methods (ranging from 96.5 to 104 kJ/mol), which

require high pressure and temperature with hydrogen gas and metal-based catalysts.

The current ODS method needs about the same amount of energy as the BDS methods, which work in milder conditions and have activation energies between 45 and 49.7 kJ/mol. However, it reacts faster and does not need to be grown with enzymes or microbes. The OBR also makes mixing and mass transfer stronger, which are often problems in BDS systems. The current study shows a good balance of low activation energy, improved mass transfer, and green catalytic chemistry, making it a sustainable and scalable alternative to traditional HDS and cutting-edge BDS technologies.

CONCLUSION

This study used a three-phase oscillatory baffled reactor (OBR) in conjunction with a vanadium pentoxide (V₂O₅)-impregnated bentonite catalyst to successfully introduce and validate a novel, non-extensive oxidative desulphurisation (ODS) method for kerosene. The V₂O₅/bentonite system’s structural stability and

Table 5 Comparison with other desulphurisation techniques for kerosene

Method	Sulphur compound	Techniques	Oxidant / Catalyst	Kinetic model	Activation energy (kJ/mol)	Reference
ODS	DBT	Batch reactor (Un-catalysed)	H ₂ O ₂ / None	-r = k CDBT	89.7	[20]
ODS	DBT	Batch reactor (Un-catalysed)	H ₂ O ₂ / None	First-order (estimated)	85.0	[21]
ODS	DBT	Photocatalysis	TiO ₂ / UV Light	Pseudo-first order	~30	[24]
ODS	DBT	Liquid-liquid extraction	Deep eutectic solvent (DES) based	Empirical	-	[25]
HDS	DBT	Trickled bed reactor	Co-Mo/Al ₂ O ₃ + H ₂	-r = k CDBT	96.5	[26]
HDS	DBT	Fixed bed reactor	Ni-Mo/γ-Al ₂ O ₃ + H ₂	Langmuir-Hinshelwood	104	[27]
ODS	DBT	Fixed-bed flow reactor	t-BuOOH / (Mo/Al ₂ O ₃)	-r = k CDBT	28 ± 1	[28]
ODS	DBT	Autoclave	Air / activated carbon-merox	-r = k CRSH2.322	25.250	[29]
ODS	DBT	Tubular with a magnetic stirrer	H ₂ O ₂ / Formic acid	-r = k CDBT	59.8	[30]
BDS	DBT	Aqueous-phase reactor	Rhodococcus erythropolis IGTS8	Monod kinetics	49.7	[31]
BDS	DBT	Resting cell assay	Gordonia alkanivorans	-	45	[32]
ODS	DBT	OBR	H ₂ O ₂ / (V ₂ O ₅ -Bentonite)	-r = k _{CDBT} ²	46.39	Present study

catalytic compatibility were validated by thorough characterisation, which also showed that the catalyst maintained high functionality even after impregnation, a crucial sign of robust active site performance. With a notable sulphur removal efficiency of 81.73% under ideal conditions (50°C, $Re_o = 382.8$, initial sulphur content = 578 ppm), the catalytic system demonstrated exceptional desulphurisation activity, underscoring the advantageous relationship between reactor hydrodynamics and catalyst performance. Additionally, dibenzothiophene (DBT) oxidation followed a second-order kinetic model with a remarkably low activation energy of 46.39 kJ/mol, highlighting the catalytic pathway's high intrinsic reactivity and efficiency in mild conditions. Based on these results, the OBR-based ODS process is positioned as a scalable energy-efficient substitute for traditional desulphurisation technologies, showing the feasibility of the suggested approach for producing cleaner Fuel.

REFERENCES

- [1] J.M. Campos-Martin, M.C. Capel-Sanchez, P. Perez-Presas, and J.L.G. Fierro, "Oxidative processes of desulphurisation of liquid fuels", *J Chem Technol Biotechnol*, vol. 85, no. 7, pp. 90-879, 2010, doi:10.1002/jctb.2371
- [2] P. Gupta, A. Kumar, and A. Singh, "Advances in oxidative desulphurisation: Catalyst design and process intensification", *Fuel Process Technol.*, vol. 220, p. 106899, 2021.
- [3] L. Wang, J. Yang, and H. Zhang, "Bentonite-supported catalysts for oxidative desulphurisation: A review", *Appl Clay Sci.* vol. 182, p. 105286, 2019.
- [4] A.M. Al-Lal, M.B. Al-Tamer, and R.P. Aranda, "Oxidative desulphurisation of fuel oils using hydrogen peroxide and heterogeneous catalysts", *Fuel Process Technol.* vol. 215, p. 106716, 2021.
- [5] International Energy Agency (IEA). "Renewables 2023 – Analysis and forecast to 2028", *Paris: IEA*; 2023. [Online] Available: <https://www.iea.org/reports/renewables-2023>
- [6] F. Boshagh, M. Rahmani, and W. Zhu, "Recent Advances and Challenges in Developing Technological Methods Assisting Oxidative Desulfurization of Liquid Fuels: A Review", *Energy & Fuels*, 2022.
- [7] X. Ma, A. Zhou, and C. Song, "A novel method for oxidative desulfurization of liquid hydrocarbon fuels based on catalytic oxidation using molecular oxygen coupled with selective adsorption", *Catalysis Today*, vol. 123, no. 1–4, pp. 276–284, May 2007, doi:10.1016/j.cattod.2007.02.036.
- [8] J. Zhang, A. Wang, X. Li, and X. Ma, "Oxidative desulphurisation of dibenzothiophene and diesel over [Bmim]₃PMo₁₂O₄₀", *Journal of Catalysis*, vol. 279, pp. 269-275, 2011.
- [9] S. Mitra, S.M. Racha, B. Shown, S. Mandal, and A.K. Das, "New insights on oxidative desulphurisation for low sulphur residual oil production", *Sustain Energy Fuels*, vol. 7, no. 1, pp. 9-270, 2023.
- [10] C. Shen, Y. J. Wang, J. H. Xu, and G. S. Luo, "Oxidative desulphurisation of DBT with H₂O₂ catalysed by TiO₂/porous glass", *Green Chem.*, 18, pp. 771-781, 2016.
- [11] D.A. Long, "Infrared and Raman characteristic group frequencies. Tables and charts George Socrates John Wiley and Sons, Ltd, Chichester, Third Edition, 2001", *J. Raman Spectrosc.* vol. 35, no. 10, p. 905, 2004, doi:10.1002/jrs.1238
- [12] A.M.Y. Jaber and H.H. Hammud, "FTIR characterisation of clay minerals and organo-modified clays: A review", *Appl Clay Sci.*, vol. 208, p. 106130, 2021.
- [13] M. Abdouss, N. Hazrati, A.A.M. Beigi, A.A. Vahida, and A. Mohammadalizadeh, "Effect of the structure of the support and the aminosilane type on the adsorption of H₂S from model gas", *RSC Adv.*, vol. 4, pp. 45-6337, 2014.
- [14] V.G. Baldovino-Medrano, V. Niño-Celis, and R.I. Giraldo, "Systematic analysis of nitrogen adsorption-desorption isotherms for microporous–mesoporous aluminosilicates", *J Chem Eng Data*, vol. 68, no. 9, pp. 28-2512, 2023, doi:10.1021/acs.jced.3c00257
- [15] W. Li, C. Wang, Z. Chen, and H. Liu, "Novel polyoxometalate-based ionic liquid catalysts for oxidative desulphurisation of diesel fuels", *Fuel*, vol. 317, p. 123414, 2022, doi:10.1016/j.fuel.2022.123414
- [16] S. A. Abdulhadi and H. H. Alwan, "Oxidative desulphurization of model fuel using a NiO-MoO₃ catalyst supported by activated carbon: Optimization study", *South African Journal of Chemical Engineering*, vol. 43, pp. 190–196, 2022, doi:10.1016/j.sajce.2022.10.010.

- [17] D. Zhao, W. Zhu, C. Ma, "Insights into the mechanism of oxidative desulphurisation with carboxylic acids and H₂O₂: A combined experimental and DFT study" *Chem Eng J.*, vol. 426, p. 130778, 2021, doi:10.1016/j.cej.2021.130778
- [18] Y. Voloshin and A. Lawal, "Kinetics of hydrogen peroxide reduction by hydrogen in a microreactor" vol. 353, pp. 9-16, 2009.
- [19] H. Luo, Y. Gu, D. Liu, and Y. Sun, "Advances in Oxidative Desulfurisation of Fuel Oils over MOFs-Based Heterogeneous Catalysts". *Catalysts*, vol. 11, no. 12, pp. 1557, 2021, doi: 10.3390/catal11121557
- [20] P.S. Kulkarni and C.A.M. Afonso, "Deep desulphurisation of diesel fuel using ionic liquids: current status and future challenges", *Green Chem.*, vol. 12, pp. 1139-1149, 2010, doi.org/10.1039/c002113j
- [21] M. Gan, G. Yang, Z. Wang, X. Sui, and Y. Hou, "Highly Efficient Oxidative Desulphurisation Catalysed by a Polyoxometalate/Carbonized Cellulose Nanofiber Composite", *Energy & Fuels*, vol. 34, no. 1, pp. 778-786, 2020.
- [22] K.V.K. Boodhoo, A.P. Harvey, "Process intensification technologies for green chemistry", *Weinheim: Wiley-VCH*; 2013.
- [23] R. Gao, X. Zhou, and X. Wang, "Recent advances in catalytic oxidative desulphurisation using deep eutectic solvents as media or additives", *Chem Eng J.*, vol. 435, p. 134890, 2022, doi:10.1016/j.cej.2022.134890
- [24] J.J.C. Bocanegra, E.E. Mora, and G.I.C. González, "Encapsulation in ceramic material of the metals Cr, Ni, and Cu contained in galvanic sludge via the solidification/stabilization method," *Journal of Environmental Chemical Engineering*, vol. 5, no. 4, pp. 3834-3843, 2017, doi:10.1016/j.jece.2017.07.044.
- [25] J. Zhao, B. Wang, R. Wang, I.V. Kozhevnikov, and K. Vladimir K. "Efficient diesel desulphurisation by novel amphiphilic polyoxometalate-based hybrid catalyst at room temperature", *Molecules*, vol. 28, no. 6, p. 2539, 2023.
- [26] S. Shawky, N.H. Shalaby, D.R.A. El-Hafiz, S. Said, M.H. Helal, and S.K. Mohamed, "Preparation of V₂O₅@ mesoporous silica sphere for novel dual oxidative-adsorptive desulphurisation", *Egypt. J. of Appl. Sci.*, vol. 35, no. 9, 2020.
- [27] B.S. Ahmed, L.O. Hamasalih, K.H.H. Aziz, Y.M. Salih, F.S. Mustafa, and K.M. Omer, "Efficient oxidative desulphurisation of high-sulphur diesel via peroxide oxidation using citric, pimelic, and α-ketoglutaric acids", *Separations*, vol. 10, no. 3, p. 206, 2023.
- [28] A.M. Nasir, J.S. Lim, F.N. Ani, R. Mat, "Photocatalytic oxidative desulfurisation of model oil using BiVO₄ under visible light irradiation", *J Environ Chem Eng.*, vol. 7, no. 1, p. 102877, 2019, doi:10.1016/j.jece.2018.102877
- [29] V.O. DJGP, L.F. Zubeir, A.V.D. Bruinhorst, M.A.A. Rocha, and M. C. Kroon, "DES as green solvents for extraction", *Green Chem.*, vol. 21, no. 15, pp. 10-4002, 2019.
- [30] M.S. Rana, V. Sámano, J. Ancheyta, and J.A.I. Diaz, "A review of recent advances on process technologies for upgrading of heavy oils and residua", *Fuel*, vol. 86, no. 9, pp. 1216-1231, 2007.
- [31] I.V. Babich and J.A. Moulijn, "Science and technology of novel processes for deep desulphurisation of oil refinery streams", *Fuel.*, vol. 82, no. 6, pp. 31-607, 2003.
- [32] A.A. Nuhu, "Bio-catalytic desulphurisation of fossil fuels: a mini review," *Rev Environ Sci Biotechnol*, vol. 12, pp. 9-23, 2013, doi: 10.1007/s11157-012-9267-x